Refined Modeling of the Entire Fatigue Process for High Quality Welds in Steel

Tom Lassen[a] and Naman Recho[b]

[a] Agder University, Faculty of Engineering, N-4876 Grimstad, Norway
[b] Institut JLRA, University Paris VI *and* ERMESS/ EPF-Ecoles d'Ingénieurs, Sceaux, France

Abstract A Two Phase Model (TPM) for the fatigue process in welded joints is developed and calibrated. The number of cycles to crack initiation is modeled by a local strain approach using the Coffin Manson equation, whereas the propagation phase is modeled by fracture mechanics adopting the simple version of the Paris law. The model is calibrated to fit the crack initiation data for a fillet welded test series subjected to axial loading with a constant stress range of 150 MPa, and the fatigue life data for similar test series subjected to stress ranges below 105 MPa. To make the model fit all test data it is crucial to select a sufficiently low transition crack depth between the initiation phase and the propagation phase. A transition crack depth of 0.1 mm was determined. Furthermore, the material parameters in the Coffin Manson equation were determined directly from the early cracking in the weld toe for full-scale welds and not from test carried out with small-scale smooth specimens. This is essential if the model is to account for the actual surface condition at the weld toe. The model is capable of taking into account the effect of the global geometry of the joint, the local weld toe geometry, applied stress ratio and the residual stress condition. S-N curves are obtained and the practical consequences of the predictions made by the TPM with respect to allowable service stresses and inspection strategies are discussed.

1 INTRODUCTION

Fatigue durability is of major concern in dynamically loaded welded structures. Fatigue life estimates are usually carried out by the S-N method, whereas crack behaviour is described by a fracture mechanics approach. However, the fatigue behaviour of welded joints subjected to typical in-service stress levels is far more complex than conventional bi-linear S-N curves and pure fracture mechanics models predict. These models are based on tests carried out in accelerated laboratory conditions. When the stress range approaches the fatigue limit, the crack initiation period becomes a very important part of fatigue life. Based on this fact a Two Phase Model (TPM) for the fatigue process is developed and calibrated. The model includes both the crack initiation and crack propagation phase. The physical model is suggested as complementary tool to statistical based S-N curves. These curves are only valid for a given joint geometry and loading conditions. It is dangerous to extrapolate them outside the range of the data. The large amount of data pertain to accelerated laboratory condition whereas in service stresses usually are close to the fatigue limit stress region where very few tests actually are carried out. At this stress regime a reliable physical model is useful both for fatigue life predictions and to determine the damage process. The latter gives necessary information for scheduled inspection planning; we must know what crack sizes to look for at various time stages. The S-N curves which do not work with the notion of a crack cannot be of any help on this matter. Furthermore, the present model gives physical insight that statistical S-N method methods do not provide. The practical consequences of the model when it comes to design and inspection planning are illustrated and discussed.

2 MODELLING THE FATIGUE PROCESS

2.1 Basic assumptions for the model

It is assumed that the total fatigue life consists of two major phases:

$$N = N_i + N_p \tag{1}$$

The number of cycles to crack initiation N_i is modeled by a local strain approach using the Coffin Manson equation, whereas the propagation phase is modeled by fracture mechanics adopting the simple version of the Paris law. The model is calibrated to fit the fatigue behaviour of fillet welded joints where cracks emanate from the weld toe, figure 1. The model is fitted to both experimental crack growth histories at high stress ranges and to fatigue lives at any stress level. Emphasis is laid on how to determine the variable weld toe notch factor, the transition crack depth between the two phases and the material parameters. The model is valid for high quality joints where a thorough post fabrication inspection is carried out.

2.2 The propagation phase

The propagation phase is modeled by linear elastic fracture mechanics adopting the simple version of the Paris law:

$$N_p = \frac{1}{C} \int_{a_0}^{a_c} \frac{da}{\left(\Delta S \sqrt{\pi\, a}\; F(a) \right)^m} \tag{2}$$

where a_0 is the initial crack depth, a_c is the critical crack depth, whereas ΔS is the nominal stress range. C and m can be regarded as material parameters. The expression in the denominator of the integral is the Stress Intensity Factor Range raised to a power of m. This type of modeling has matured into the application stage and guidance on the choice of model and parameters is given in Ref.1. Hence, description of this model is not emphasized in the present article. The present work focuses on the development and calibration of a model for the initiation part of the fatigue life.

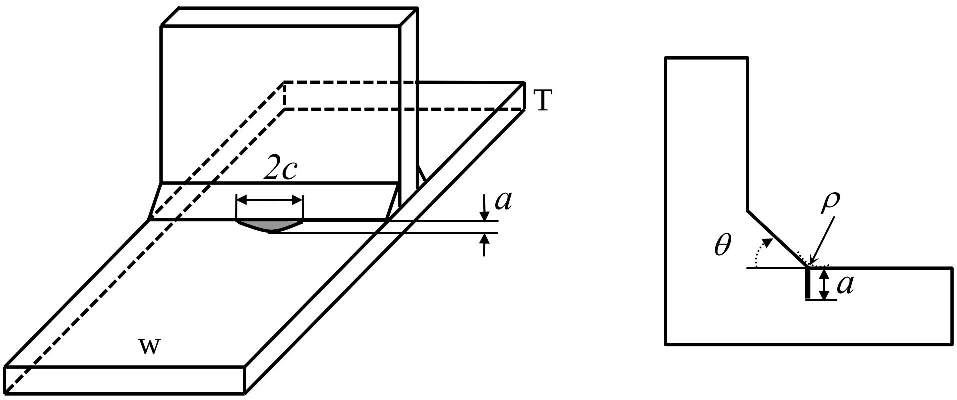

Figure 1. Typical joint configuration and definition of crack shape

2.3 Modeling the fatigue crack initiation period

2.3.1 Basic concept and equations for the local stress-strain approach

The predictions for the number of cycles to crack initiation, N_i, are based on the Coffin- Manson equation with Morrow's mean stress correction (Refs. 2, 3):

$$\frac{\Delta\varepsilon}{2} = \frac{\left(\sigma'_f - \sigma_m\right)}{E} \left(2\, N_i\right)^b + \varepsilon'_f \left(2\, N_i\right)^c \tag{3}$$

Here $\Delta\varepsilon$ is the local strain range and σ_m is the local mean stress at the weld toe. The parameters b and c are the fatigue strength and ductility exponents, and σ'_f and ε'_f are the fatigue strength and ductility coefficients respectively. The local stress and strain behavior is given by the Ramberg-Osgood stabilized cyclic strain curve:

$$\Delta\varepsilon = \frac{\Delta\sigma}{E} + 2\left(\frac{\Delta\sigma}{2\, K'}\right)^{\frac{1}{n'}} \tag{4}$$

where K' and n' are the cyclic strength coefficient and strain hardening exponent respectively. Equation 4 is combined with the Neuber rule:

$$\Delta\varepsilon\; \Delta\sigma = \frac{\left(K_t\; \Delta S\right)^2}{E} \tag{5}$$

where ΔS is the nominal stress range, E is the Young modulus and K_t is the stress concentration factor at the welded toe. The following expression for K_t is used (Ref. 4):

$$K_t = 1 + \left[0.5121 \; (\theta)^{0.572} \left(\frac{T}{\rho} \right)^{0.469} \right] \tag{6}$$

where θ is the weld toe angle (radians) and T is the plate thickness, see Figure 1.
The definition of the local stress-strain variation is illustrated in Fig. 2. The nominal stress S (left) and the local stress σ (right) are shown for the first reversal (0-1) and the stabilized hysteresis loop (1-2-3). The local $\Delta\sigma$ and $\Delta\varepsilon$ and the mean stress, σ_m, corresponding to the cyclic loading, are determined. The effect of cyclic hardening or cyclic softening is neglected.

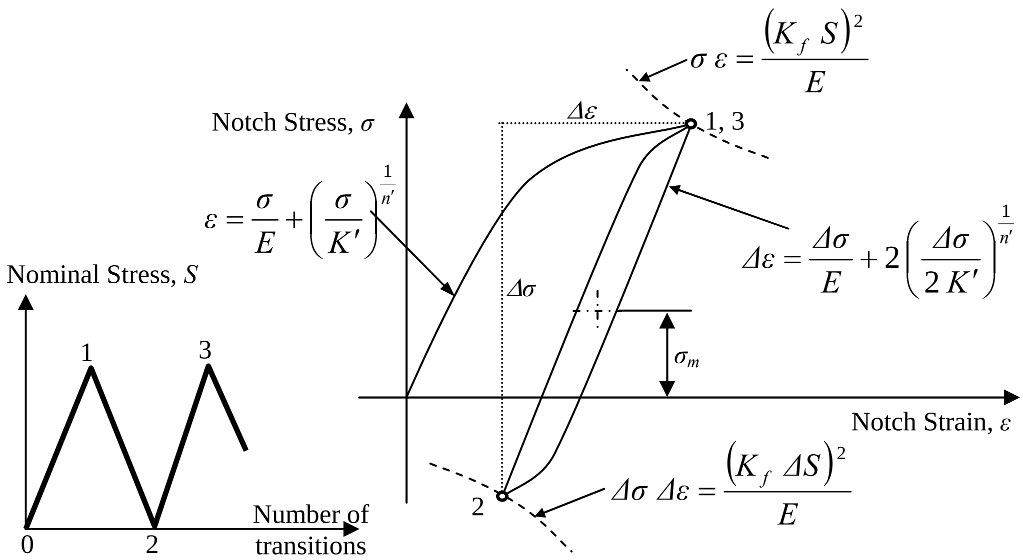

Figure 2. Schematic illustration of the local stress-strain hysteresis loop analysis.

2.3.2 The problem of determining important parameters

When applying the Coffin-Manson approach to predict time to crack initiation at the weld toe, three questions arise. The first is what stress concentration factor K_t one should choose to characterize the notch effect from the highly variable local toe geometry. The next is the definition of time to crack initiation, i.e. what crack depth is reached at the end of the phase before propagation is considered to take over. This depth will be referred to as the transition depth. If this depth is chosen too large, the initiation phase will not obey Equation 3 due to a substantial amount of crack growth involved. Several definitions are possible for the transition depth and this is probably one of the reasons why so few two-phase models have been applied in practice. The last question is how to determine the cyclic mechanical parameters and the parameters in the Coffin-Manson equation such that they are valid for the weld toe condition. Usually these parameters are determined from tests with small-scale smooth specimens. However, in a full-scale weld there may be size effects and surely surface finish effects involved. Tests with smooth specimens may not be representative for the rough surface conditions found in the vicinity of the weld toe. It is our hypothesis that the actual parameters should be determined directly from full-scale tests with welded joints where the early cracking is measured. Based on the discussion above we will emphasize three issues:

- Local toe geometry and stress concentration factor
- The choice of the transition depth
- The determination of the parameters in Coffin-Manson law

The decisions taken regarding these three issues are based on two large data basis. The life data for these tests series are plotted in figure 4. We shall explain this figure more in detail later. The test series carried out at a stress range of 150 MPa shall be referred to test series 1. For this test series, the time to crack initiation was measured as well as the variations found in local toe geometry, Ref. [5]

2.3.3 Local toe geometry and stress concentration factor

The statistics for the local geometry for the specimens tested in series 1 (database 1) are characterized by a mean value of 58 degrees for the flank angle and 1.3 mm for the toe radius. If we substitute the values into

Equation 6 this will give K_t = 2.9. This value is corroborated by a refined finite element analysis. However, it is highly likely that the cracks initiate at a more unfavorable geometry. It is above all the variability in the toe radius that yields K_t values in the range from 2.9 and up to 7. If the radius at an arbitrary locus along the weld seam is treated as a stochastic variable, the extreme value distribution for the smallest value will read:

$$1 - F_{\rho\min}(\rho) = \left(1 - F_{\rho}(\rho)\right)^{k} \tag{7}$$

where $F_\rho(\rho)$ is the Cumulative Distribution Function (CDF) of the an arbitrary radius whereas $F_{\rho\min}(\rho)$ is the CDF for the smallest value over the length *W, see figure 3*. The integer k is the number of uncorrelated radii along the weld seam. The mean and peak values for this smallest radius can be derived from the corresponding Probability Density Function (PDF). The peak value is by definition the most likely value for the smallest radius within the length *W*. In the present case (W=60 mm, k=10) the extreme toe radius was close to 0.4 mm which correspond to SCF= 4.5. This figure will be used in our calculations. For longer seams, $F_\rho(\rho)$ will remain the same, whereas $F_{\rho\min}(\rho)$ will shift towards left in figure 3, i.e. the minimum radius will decrease.

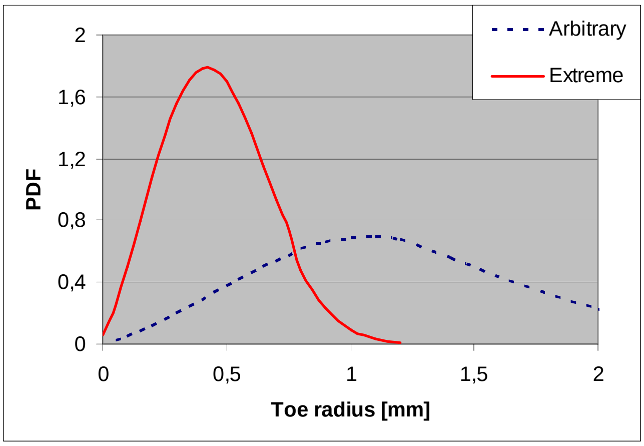

Figure 3. Definition of the toe notch geometry in one specimen by extreme value statistics

2.3.4 Transition depth

Lawrence et al., (Ref. 3) suggested that the transition depth should be between 0.05 and 0.1 mm. The following arguments support a transition depth of 0.1 mm:

- To apply the facture mechanics model at crack depths smaller than 0.1 mm may be dubious because one approaches the grain size of the steel (typically 0.01 mm).
- In laboratory tests it is hardly possible to measure any crack less than 0.1 mm with sufficient accuracy without using destructive methods.
- Cracks with a depth below 0.1 mm are not of interest in in-service inspection as no common NDI method can detect such small cracks. Hence, for inspection planning we do not need the notion of a crack smaller than 0.1 mm.

As can be seen, our arguments are partly theoretical, partly practical. The main criterion is however that the model is capable of predicting the entire fatigue life at any stress level (Data base 1 and data base 2)

2.3.5 Cyclic mechanical properties and parameters in Coffin-Manson equation

It is our hypothesis that parameters determined from small-scale smooth specimens are not directly applicable for weld toe conditions. Hence, we will determine these parameters directly from the time to early cracking measured for test series 1. For this test series, the number of cycles spent to reach a crack depth of 0.1mm was 30 % of the entire fatigue life plotted in figure 4. We now seek the parameters in Equations 3 and 4 that correspond to this initiation time. The calibration is carried out by assuming a dependency between the various parameters with the Brinell Hardness (*HB*) as the key parameter. The applied relations are given in equations 8 (Ref. 6). S_u and S_y are the tensile stress and yield stress respectively, and S_y' is the cyclic yield stress. An absolute value of HB is sought such that the time to reach a given transition crack depth coincides with what actually has been measured on the welded joints in database 1. The solution gives a *HB* close to 202 for the cycles to reach a crack depth 0.1 mm. This *HB* is very close to the value actually measured in the HAZ of the weld toe. The values measured for the base metal was *HB* = 145 and values of the HAZ was 213. Hence, our solution is only 5% less than the highest value measured at the potential crack locus. The corresponding parameters are given in table 1.

$$S_u = 3.45\ HB \quad \text{MPa}$$

$$S'_y = 0.608\ S_u \quad \text{MPa}$$

$$b = -0.1667\ \log\left(2.1 + \frac{917}{S_u}\right)$$

$$c = -0.7 < c < -0.5$$

$$n' = \frac{b}{c}$$

$$K' = S_y (0.002)^{-n'} \quad \text{MPa}$$

$$\sigma'_f = 0.95\ S_u + 370 \quad \text{MPa} \qquad (8)$$

$$\varepsilon'_f = \left(\frac{\sigma'_f}{K'}\right)^{1/n'}$$

Table 1. Cyclic mechanical properties and parameters in the Coffin Manson equation calibrated for time to reach 0.1 mm, *HB* = 202.

Parameter, Symbol (units)	**Value**
Cyclic yield stress, S'_y (MPa)	424
Ultimate strength, S_u (MPa)	697
Young modulus, *E* (GPa)	206
Fatigue strength exponent, *b*	-0.089
Fatigue strength coefficient, σ'_f (MPa)	032
Fatigue ductility exponent *c*	-0.6
Fatigue ductility coefficient ε'_f	0.81
Cyclic strength coefficient, *K'* (MPa)	1064
Strain hardening exponent, *n'*	0.148

3 CONSTRUCTING S-N CURVES WITH THE TPM

All the important model parameters have now been determined. The local toe geometry is characterized by extreme value statistics, the fatigue initiation parameters corresponding to HB=202 are given in table 1. The transition depth is determined to 0.1 mm. These figures were used to calculate the fatigue initiation life. The propagation phase was subsequently added to calculate the entire fatigue life. The model predicts exactly the mean value for the fatigue lives of database 1 at a stress range of 150 MPa. When the stress range was decreased from 150 MPa to below 100 MPa, the model predicts fatigue lives very close to the median line of database 2, see figure 4. The median line is determined by a Random Fatigue-Limit Model, Ref. [7]. As can be seen from the figure, the constructed S-N curve is non-linear for a log-log scale.

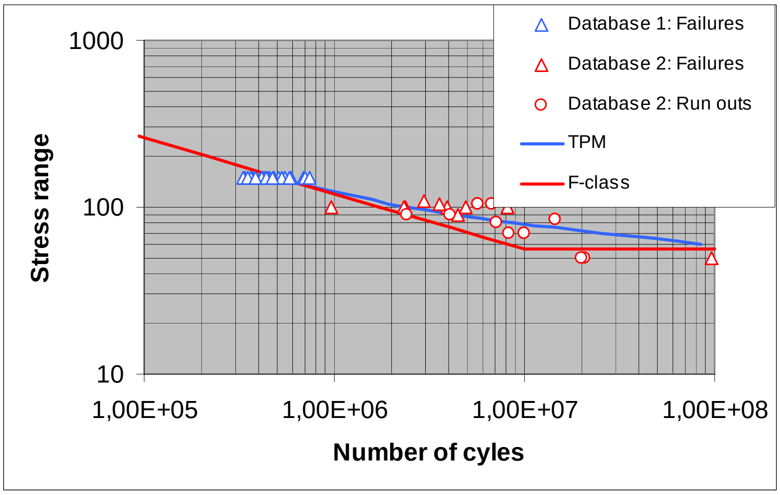

Figure 4. Constructed median S-N curve together with life data and the F-class curve

The bi-linear median F-class curve given in rules and regulations, Ref. [9], is also drawn. As can be seen the curve obtained from the present TPM model is more in accordance with the fatigue life data close to the knee point of the F-class curve. It is obvious that the conventional bi-linear F-N curve does not fit the experimental facts in the stress region just above the fatigue limit. The TPM curve fits the F-class at high and low stress levels, but not in the range just above the fatigue-limit defined by the F-class curve.

Table 2– Results derived from the TPM at various stress ranges. Stress Relieved (SR), R = 0.3.

Stress range (MPa)	N_i (cycles) TPM	N_p (cycles) TPM	N_t (Cycles) TPM	N_i/N_t % TPM	N_t RFLM	N_t F-class
150	1.4×10^5	3.3×10^5	4.7×10^5	30	4.6×10^5	5.1×10^5
120	5.6×10^5	6.5×10^5	1.2×10^6	47	1.1×10^6	1.0×10^6
100	2.1×10^6	1.1×10^6	3.2×10^6	66	2.5×10^6	1.7×10^6
80	1.6×10^7	2.2×10^6	1.8×10^7	88	11.0×10^6	3.4×10^6
60	3.7×10^8	5.1×10^6	2.9×10^8	99	∞	8.0×10^6

Another conspicuous difference between the F-class curve and the TPM curve is that the latter does not results in a fatigue limit. The obtained curve continues to decrease with a more and more shallow slope. This is in accordance with a recent work carried out in Ref. 8 where the existence of a fatigue limit is regarded as a common prejudice. The figures for the graphs in Figure 4 are given in table 2. As can be seen the initiation life at low stress ranges between 60 and 80 MPa is more than 80 % of the total fatigue life according to the TPM. These stress levels are often representative for in-service stresses, e.g. for a welded offshore structure.

4 PRACTICAL CONSEQUENCES OF THE TPM

We have constructed an *S-N* curve which is nonlinear for a log-log scale and that predicts substantially longer lives at stress ranges below 100 MPa than does the F-class linear curve. Furthermore, at these long fatigue lives (more than 5×10^6 cycles) the initiation life is at least 70% of the entire fatigue life. We will show by a simple example the practical consequences of these results with respect to:

- Predicting fatigue life for selecting dimensions of a joint
- Predicting crack growth evolution for inspection planning

We compare our results with the results obtained by the median F-class curve and a pure Fracture Mechanics Model (FMM) calibrated to make life predictions made by F-class and by the FMM coincide.

4.1 Design and dimensions

For simplicity we assume constant amplitude loading and choose a stress range in the region considered, i.e. ΔS = 80 MPa. By using the model we get the results in Table 3 for an as welded condition.

Table 3– Median life (cycles) predictions made by the TPM and the F-class (As Welded).

Stress range (MPa)	TPM			F-class or *Equivalent* FMM
	N_i	N_p	N_t	$N_t = N_p$
80	6.6×10^6	2.2×10^6	8.8×10^6	3.4×10^6
58				8.8×10^6

Compared with the figures in table 2 it is seen that the initiation period is reduced due to the fact that the joint is assumed to be in an As Welded condition. The initiation life has decreased from 88% of the total fatigue life to 75%. Hence, the residual stresses are accounted for. Details and applied data are for the model found in Refs. [1,10]. As can be seen at 80 MPa the TPM predicts 2.5 times longer fatigue life than the F-class. If dimensions are chosen according to the F-class the dimensions must be increased by 38% to give the same predicted fatigue life, i.e. 8.8×10^6 cycles. This will correspond to a permissible stress range of 58 MPa only. These assessments based on the median S-N curves will also be valid for the design curves if the lives predicted by the TPM have the same scatter as the F-class.

4.2 Predicted crack evolution and inspection planning

Let us compare the two alternatives above with respect to inspection planning. The first alternative is the TPM based design with an allowable stress of 80 MPa, the second alternative is the F-class design or the equivalent FMM design with allowable stress range 58 MPa. Our task is now to compare the crack evolutions before and up to final fracture based on the TPM and the FMM in the two cases. We shall more precisely consider the effect of a scheduled inspection program for the two crack growth histories. The purpose of such a program is of course to detect cracks so that they can be repaired before reaching the final critical crack size. We introduce the concept of a Probability of Detection (POD) curve to characterize the performance of the inspection technique. The curve is shown to the left in Fig. 5. The obtained crack growth histories for the FMM and the TPM are shown to the right. As can be seen the curve derived from the TPM has a more hidden path that makes the crack more difficult to detect at an early stage. The reliability calculations for an inspection program are carried out using a simple quasi-stochastic approach often used in the aircraft industry. We call the method quasi-stochastic because it does not take into account the randomness of the crack evolution, but applies the mean curves as given to the right in Fig. 5. If the strategy is to implement k inspections during the planned service life, the event that all of them fail can be estimated by:

$$P_F = \prod_{i=1}^{i=k} [1 - POD(a_i)] \tag{9}$$

The expression is based on the assumption that each inspection is independent. The reliability of the inspection program is $R = 1 - P_F$. If we are planning k=17 inspections at a constant time interval corresponding to 5×10^5 cycles, we will for the two curves in Fig. 5 get the figures in Table 4. As can be seen, there is an important difference in achieved reliability for the given inspection program for the two different crack evolutions. The FMM predicts a reliability of 0.999, whereas the TPM predicts only 0.935.

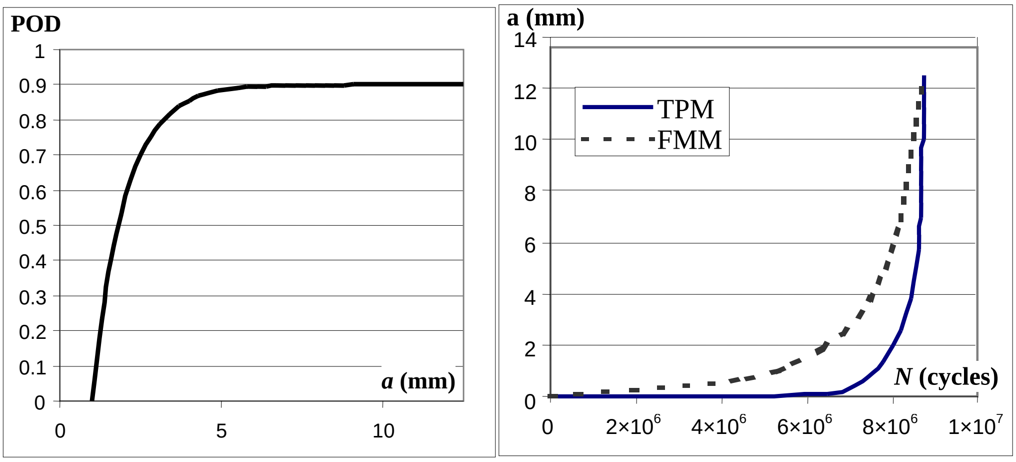

Figure 5. Left: POD curve Magnetic Particle Inspection; Right: Predicted crack evolution for FMM, ΔS = 58 MPa and TPM, ΔS = 80 MPa.

Table 4– Reliability calculations for a given inspection program.

Model for prediction	First effective inspection	Last effective inspection	Number of effective inspections	Reliability	Probability of failure
FMM	5.5×10^6	8.5×10^6	7	0.9999	1.0×10^{-4}
TPM	8.0×10^6	8.5×10^6	2	0.935	6.5×10^{-2}

When comparing the probability of failure the difference becomes more striking, the probability of failure pertaining to the FMM is normally in the acceptable range, whereas the one pertaining to the TPM is not. If the damage behavior and reliability predictions made by the TPM are accepted as true, one would obtain acceptable reliability if the inspection efforts were concentrated in the last part of the service life with a decreased inspection interval of 2×10^5 cycles. This is a consequence of the extreme long crack initiation period at this stress level. During this long incubation period the crack is miniscule and hidden. Hence, inspection efforts are a waist. As can be seen from Table 4, only the two last inspections have any probability of detecting the crack. For all the former planned inspections it is impossible to detect the crack. For a more fully probabilistic analysis the conclusion will remain the same.

5 CONCLUSIONS

The fatigue behaviour of high quality welded joints in steel is far more complex than conventional bi-linear S-N curves and pure fracture mechanics model predict. At typically low in-service stress ranges the crack initiation period, defined as time to reach a crack depth of 0.1 mm, represents the dominating part of the fatigue life. To describe this behaviour a Two Phase Model (TPM) is required.

The non-linear S-N curves obtained from the TPM coincides with the conventional S-N curve predictions at high stress levels, but fits the experimental data near the fatigue limit far better. The abrupt knee-point of the bi-linear curve does not fit the facts in this stress region.

The theoretical consequence of the model is that the fatigue limit does not exist. The long fatigue lives at low stress level are explained by an extremely long initiation period and not, as for the fracture mechanics model, by a threshold value in the stress intensity factor. The shallow surface breaking crack near the weld toe do not obey the threshold law, they tend to grow considerably faster. The TPM results in an S-N curve which continues to decrease at low stress levels but with a very shallow slope close to the b parameter in the Coffin Manson law.

The first practical consequence of the model is that it predicts considerably longer fatigue lives at low stress levels than the conventional bi-linear curves found in rules and regulations. This will results in higher permissible stresses and smaller dimensions of the joints. The second practical consequence is that a scheduled in-service inspection program should be more progressive with service time compared with programs based on a pure fracture mechanics model. This will result in a long initial inspection interval and short intervals at the end of service life.

6 REFERENCES

6.1 Books

1 Lassen, T. and Recho, N. : FLAWS : Fatigue Life Analysis of Welded Structures
ISTE, London, UK, 2006, ISBN 10: 1-905209-54-1 pp 140-193.

2 Lawrence, F. V, Dimitrakis, S. D., and Munse, W. H. 1996. Factors influencing Weldment Fatigue. *Fatigue and Fracture*, ASM Handbook, Vol. 19: pp. 274-286, Materials Park, OH.

6.2 Journal articles

3 Yung, J. Y., and Lawrence, F. V. 1985. Analytical and Graphical Aids for the Fatigue Design of

4 Niu, X., and Glinka, G. 1987. The Weld Profile Effect on the Stress Intensity Factors in Weldments. *Int. J. of Fracture* 35: pp. 3-20.

5 Lassen, T. 1990: The effect of the welding process on the fatigue crack growth in welded joints.
Welding Journal 96 (2): pp 75s, 85s

6 Testin, R. A., Yung, J. Y., Lawrence, F. V., and Rice, R. C. 1987. Predicting the Fatigue Resistance of Steel Weldments. *Welding Journal* 66: 93-s to 98-s.

7 Lassen, T., Darcis, Ph. and Recho, N.: Fatigue Behavior of Welded joint. Part 1 : Statistical modeling of the fatigue life. Welding Journal, December 2005

8 Sonsino, C.M.: Course of S-N curves especially in the high-cycle fatigue regime with regard to component design and safety-. To appear in International Journal of Fatigue during autumn 2007

6.3 Codes and regulations

9 BS 5400: Steel, concrete and composite bridges, 1980. *Part 10: Code of practice for fatigue*, London, British Standard Institution (BSI).

10 BS 7910, 2005. Guidance on Methods for Assessing the Acceptability of Flaws in Fusion Welded Structures, *London, British Standards Institution (BSI)*